Talanta 233 (2021) 122536

Contents lists available at ScienceDirect

Talanta

journal homepage: www.elsevier.com/locate/talanta

Conjugation-regulating synthesis of high photosensitizing activity porphyrin-based covalent organic frameworks for photodynamic inactivation of bacteria

Fan-Lin Meng [c], Hai-Long Qian [a,b,c,*], Xiu-Ping Yan [a,b,c,d,**]

[a] State Key Laboratory of Food Science and Technology, Jiangnan University, Wuxi, 214122, China
[b] International Joint Laboratory on Food Safety, Jiangnan University, Wuxi, 214122, China
[c] Institute of Analytical Food Safety, School of Food Science and Technology, Jiangnan University, Wuxi, 214122, China
[d] Key Laboratory of Synthetic and Biological Colloids, Ministry of Education, School of Chemical and Material Engineering, Jiangnan University, Wuxi, 214122, China

ARTICLE INFO

Keywords:
Conjugation
Photosensitizing activity
Porphyrin-based covalent organic frameworks
Photodynamic inactivation

ABSTRACT

Preparation of porphyrin-based covalent organic frameworks (Por-COFs) with high photosensitizing activity for photodynamic inactivation of bacteria is of great challenge, but significant for economy and human health. Herein, we show a conjugation-regulating strategy to design and synthesize Por-COFs with high photosensitizing activity for the photodynamic inactivation of bacteria. Terephthalaldehyde (Da), 2,5-Dihydroxyterephthalaldehyde (Dha), and 2,5-Diethoxyterephthalaldehyde (Deta) with different conjugation degrees are selected to condense with 5,10,15,20-Tetrakis(4-aminophenyl)porphyrin (Tph) to synthesize COF-366, DhaTph, and JNU-2, respectively. The higher conjugation of Dha and Deta than Da leads to the higher conjugation of DhaTph and JNU-2, respectively. Moreover, the hydroxyl group in Dha and the ethoxy group in Deta further expand the conjugation of DhaTph and JNU-2 via the formation of intralayer extended π-cloud delocalization and p-π conjunction, respectively. The extension of conjugation for DhaTph and JNU-2 results in the increase of inter-system crossing process and significantly improves their photosensitizing activity. Furthermore, JNU-2 with the highest photosensitizing activity exhibits superior antibacterial effects toward *Staphylococcus aureus* (99.1%) and *Escherichia coli* (96.8%). This study offers a new conjugation-regulating strategy for designing high photosensitizing activity of Por-COFs for the inactivation of bacteria.

1. Introduction

Bacteria cause food spoilage, foodborne diseases, pneumonia and wound infections, and render a constant threat to public health and significant impediment to socio-economic development [1,2]. Efficient bacteria inactivating methods are of extreme importance to economy and human health. As one of the most common sterilization, antibiotic therapy leads to serious worldwide healthy issue of drug resistance [3,4]. Photodynamic inactivation is a promising candidate of sterilization due to its efficiency, broad-spectrum and no drug resistance [5]. The photosensitizer in photodynamic inactivation produces efficient reactive oxygen species (ROS) to give a multi-targeted damage to living tissues including bacteria, viruses, and fungi under the excitation of a certain wavelength light in the presence of O_2 [6].

Photosensitizer plays a key role in photodynamic inactivation due to its production of ROS. Over decades, various photosensitizers have been reported such as phenothiazinium dyes (methylene blue, toluidine blue O), naturally occurring photosensitizer (chlorophylls, psoralens and perylene quinonoid pigments), and tetrapyrroles (porphyrins, phthalocyanines, chlorins and bacteriochlorin) [7,8]. However, these photosensitizers mainly suffer from self-aggregation in solution, which highly diminishes their photosensitizing activity [9–11]. A competent approach to overcome the self-aggregation is the synthesis of solid photosensitizer with ordered porous structure to immobilize photosensitizer unit with a forced and well-defined arrangement. Moreover, the ordered structure with high porosity provides photosensitizers a good access to O_2, leading to highly efficient conversion of O_2 to ROS [12].

Covalent organic frameworks (COFs) are a class of porous crystalline

---

* Corresponding author. State Key Laboratory of Food Science and Technology, Jiangnan University, Wuxi, 214122, China.
** Corresponding author. International Joint Laboratory on Food Safety, Jiangnan University, Wuxi, 214122, China.
E-mail address: hlqian@jiangnan.edu.cn (H.-L. Qian).

https://doi.org/10.1016/j.talanta.2021.122536
Received 24 April 2021; Received in revised form 11 May 2021; Accepted 15 May 2021

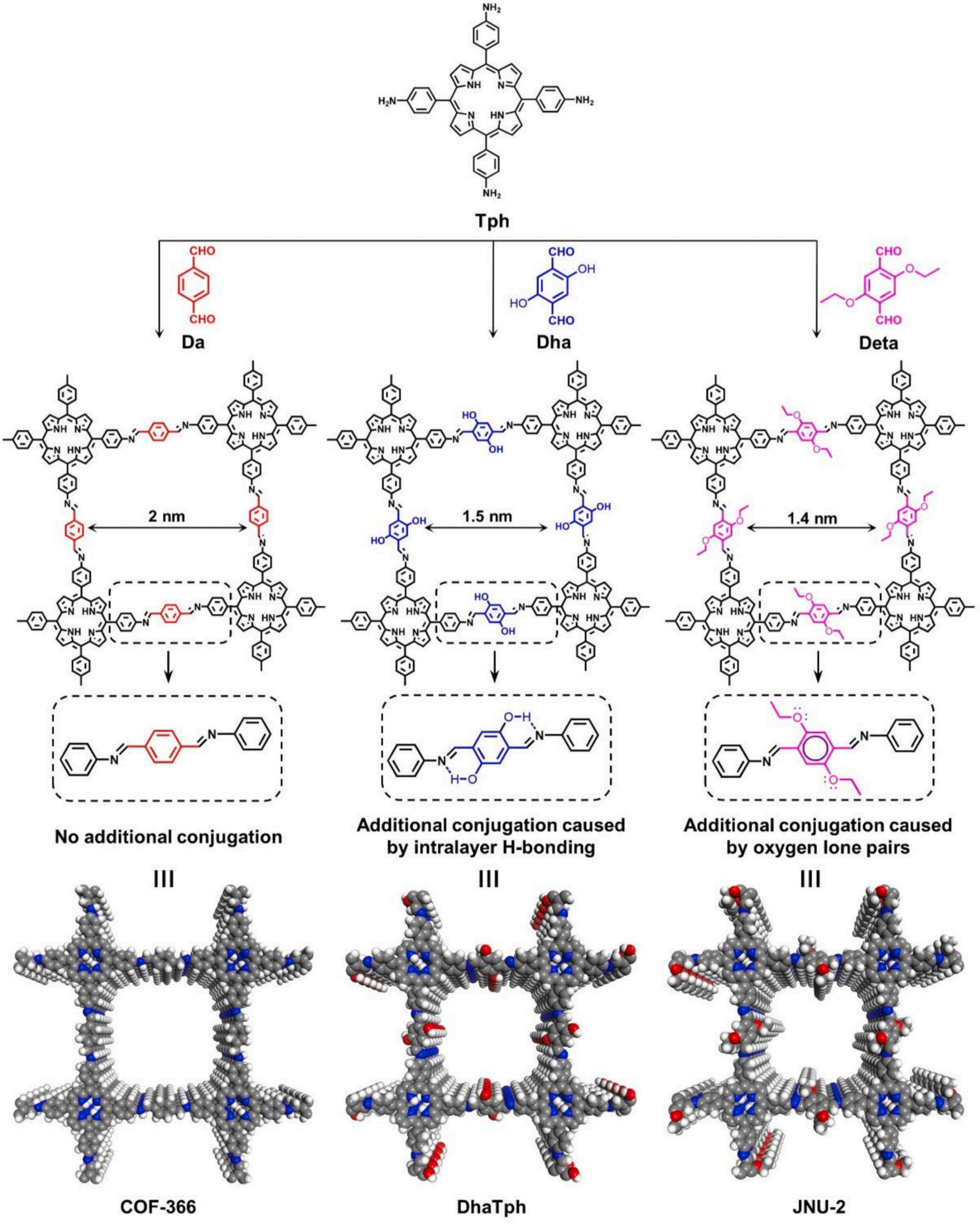

Fig. 1. Design and synthesis of Por-COFs via the conjugation-regulating strategy. Inset: the edge units of Por-COFs with corresponding conjugation effect (COF-366 with no additional conjugation as the control; DhaTph with additional conjugation from the intralayer H-bonding; JNU-2 with additional conjugation from the oxygen lone pairs). The C, N, O and H atom were represented with in grey, blue, red white in graphic view of Por-COFs, respectively. (For interpretation of the references to colour in this figure legend, the reader is referred to the Web version of this article.)

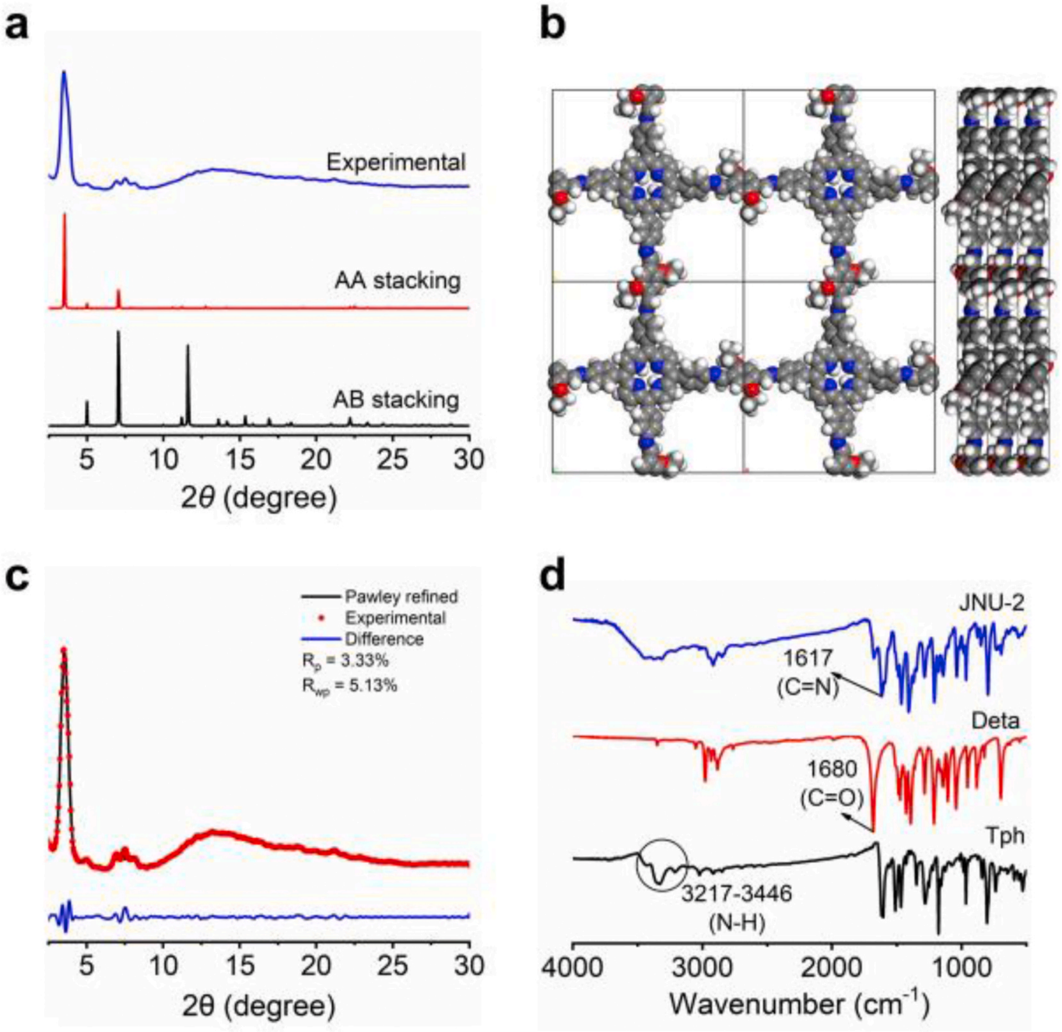

Fig. 2. (a) Experimental and simulated PXRD patterns of JNU-2. (b) Unit-cell structure of AA-stacking mode of JNU-2. (c) Pawley refinement of JNU-2. (d) FTIR spectra of Deta, Tph and JNU-2.

materials consisting of organic building with covalent bonds, and show wide applications in various fields [13–18]. Porphyrins are promising building monomers for photosensitizing COFs due to their planar and rigid geometry with inherent functionalities involving photosensitizing and redox-active properties. A few porphyrins-based COFs (Por-COFs) have been developed for photocatalytic, electrocatalytic, sensing, and semiconducting applications [19–23]. The special features of high crystallinity, permanent porosity, and ordered columnar π-arrays of Por-COFs also qualify them as excellent photosensitizer for photodynamic inactivation of bacteria. The conjugation degree of photosensitizer shows high effect on the intersystem crossing (ISC) between excited singlet (S) and triplet states (T), relating to ROS generation capabilities [24,25], but have not been explored for the preparation of high photosensitizing activity of Por-COFs for photodynamic inactivation of bacteria.

Herein, we report a conjugation-regulating strategy for the design and synthesis of Por-COFs with high photosensitizing activity in photodynamic inactivation of bacteria. As the building monomer greatly affects the conjugation of COFs, Terephthalaldehyde (Da), 2,5-Dihydroxyterephthalaldehyde (Dha), and 2,5-Diethoxyterephthalaldehyde (Deta) with different conjugation degrees are selected to condense with 5,10,15,20- Tetrakis(4-aminophenyl)porphyrin (Tph) to synthesize Por-COFs (COF-366, DhaTph, and JNU-2). The preparation, characterization, and photosensitizing activity of Por-COFs are detailly investigated as well as their mechanism of the conjugation-regulating for photosensitizing activity. The highly ordered Por-COFs with excellent singlet oxygen efficiencies are applied to show their high potential in photodynamic inactivation of bacteria.

2. Results and discussion

2.1. Design and preparation of Por-COFs

Fig. 1 shows the design and preparation of Por-COFs via the conjugation-regulating strategy. The specific wavelength light directs the conversion of photosensitizer electron from the ground state (S_0) to S. Part of electron in S will covert to T via ISC. The released energy from T_1 to S_0 converts the surrounding O_2 into ROS [6]. Therefore, the core for the preparation of high photosensitizing activity of Por-COFs is to increase the ISC. The extension of Por-COFs conjugation is expected to an efficient way to promote the ISC [26–29], but have not been explored for the preparation of high photosensitizing activity of Por-COFs. The conjugated monomers could increase the conjugation of two-dimensional (2D) materials after the formation of two-dimensionally extended π-conjugated structure [30–32]. Here, we select three monomers Da, Dha and Deta with different conjugation degrees for the condensation with Tph to regulate the conjugation of Por-COFs. The corresponding Por-COFs COF-366, DhaTph, and JNU-2 with ideal ordered crystalline structure were obtained by optimizing solvent, temperature, and time (Fig. S1-S11). The COF-366 with no

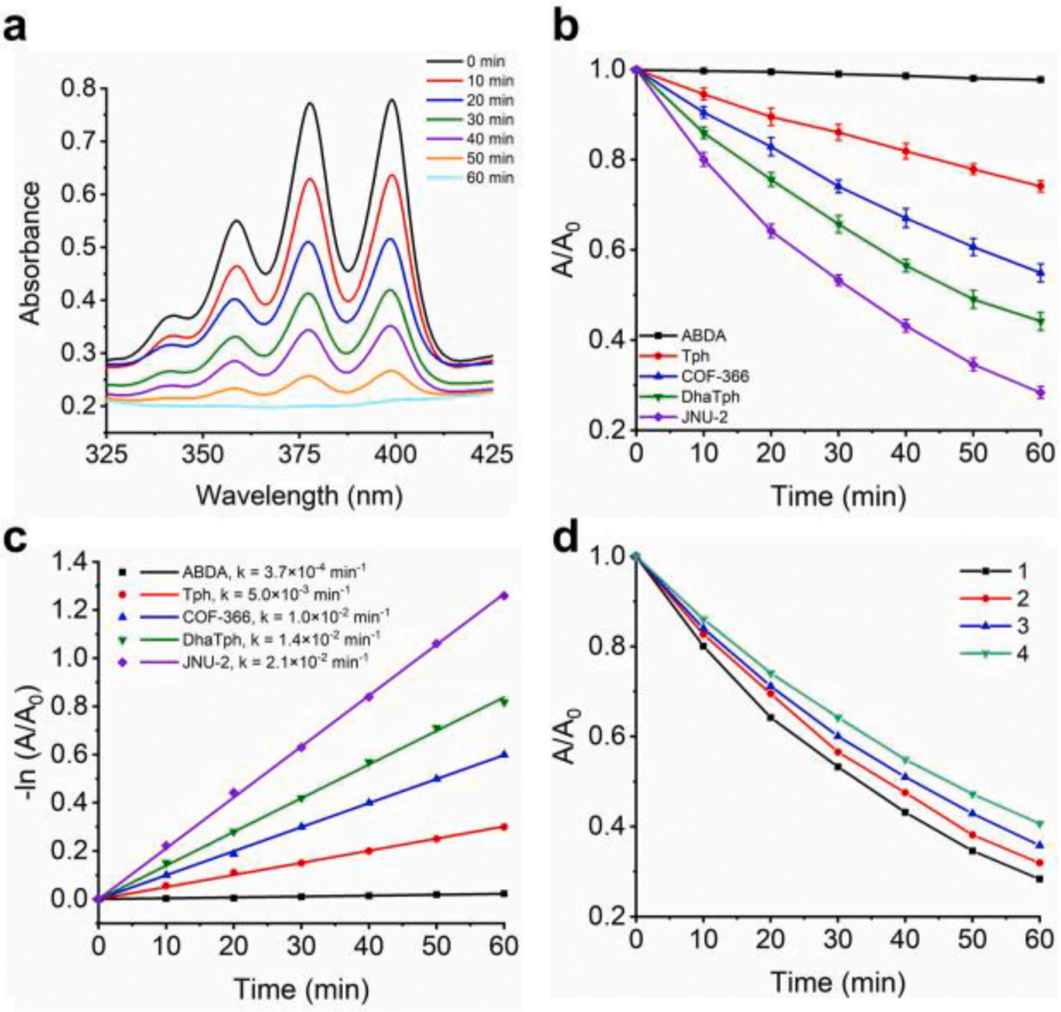

Fig. 3. (a) Change in the UV–vis absorption spectra of ABDA in the presence of JNU-2 with irradiation time. (b) Time-dependent degradation of ABDA at 379 nm caused by the singlet oxygen produced from Por-COFs and Tph. (c) Pseudo-first-order kinetic curves for ABDA degradation of Por-COFs and Tph. (d) Time-dependent degradation of ABDA at 379 nm caused by the singlet oxygen produced from JNU-2 in different runs.

additional regulation of conjugation was prepared as the control Por-COFs to show the efficiency of our strategy. The extension conjugation of DhaTph, and JNU-2 via the control of monomer intend to favour the increase of the photosensitizing activity of Por-COFs.

2.2. *Characterization of Por-COFs*

The crystallinity of prepared Por-COFs was characterized by powder X-ray diffraction pattern (PXRD). The main characteristic peaks of PXRD for the as-prepared COF-366 and DhaTph at 3.5° and 6.9°match well with the those reported for their corresponding COFs [29,33], verifying the synthesis of two COFs (Fig. S12). The PXRD pattern of new COF JNU-2 shows characteristic peaks at 3.5°, 5.0°, 6.9°, 7.5°and 8.1°, indicating its ordered crystalline structure (Fig. 2a). Possible 2D models with AA and AB stacking layer were built to clarify the structure of JNU-2 (Fig. 2b; Fig. S13). The experimental PXRD pattern of JNU-2 is in good agreement with that of the AA stacking model, but differs from that of AB stacking mode, demonstrating that JNU-2 adopts the AA stacking mode with pawley refined P1 unit cell ($a = b = 24.93$ Å, $c = 3.99$ Å, $\alpha = \beta = \gamma = 90°$) rather than the corresponding AB stacking model (Fig. 2a and c and Table S1).

The lack of the stretching bands of the amino (3217-3446 cm^{-1}) and aldehyde (1667-1680 cm^{-1}) in the original building monomers as well as the concomitant presence of imine (1610-1617 cm^{-1}) stretching band in Fourier transform infrared (FTIR) spectra of Por-COFs reveal the successful reaction of Tph and aldehyde monomer (Fig. 2d; Fig. S14-S15). Compare with COF-366, the intralayer hydrogen bonding between imine and hydroxyl groups of DhaTph gave the C═N vibration band a shift from 1613 to 1610 cm^{-1}. The oxygen lone pairs of the electron donating ethoxy in JNU-2 resulted in a shift of the C═N vibration band from 1613 to 1617 cm^{-1} (Fig. S16) [34,35].

The porosity of Por-COFs was assessed by the analysis of their N_2 adsorption isotherms. The prepared COF-366, DhaTph and JNU-2 gave the Brunauer–Emmett–Teller (BET) surface areas of 214, 830, and 328 m^2 g^{-1} and the total pore volumes of 0.370, 0.583, and 0.475 cm^3 g^{-1}, respectively (Fig. S17-19). The improved surface areas of DhaTph and JNU-2 were contributed to the formation of strong intralayer hydrogen bonding and the decrease of the intralayer repulsion via the introduction of oxygen lone pairs, respectively. The average pore-sizes of COF-366, DhaTph, and JNU-2 were 2.0, 1.5, 1.4 nm, respectively, and sufficient for the access of O_2. Scanning electron microscopy showed the sheet-like morphology of all the three Por-COFs (Fig. S20-S22).

The crystallinity and the skeleton of Por-COFs remained after treatment with tetrahydrofuran (THF), dimethylformamide (DMF), 0.01 M Phosphate buffer saline (PBS) buffer, 0.1 M HCl and 0.1 M NaOH for 1 day due to no obvious change in their PXRD patterns (Fig. S23-S25). These results confirmed that the prepared Por-COFs possessed high chemical stability for future application. Thermogravimetric analysis

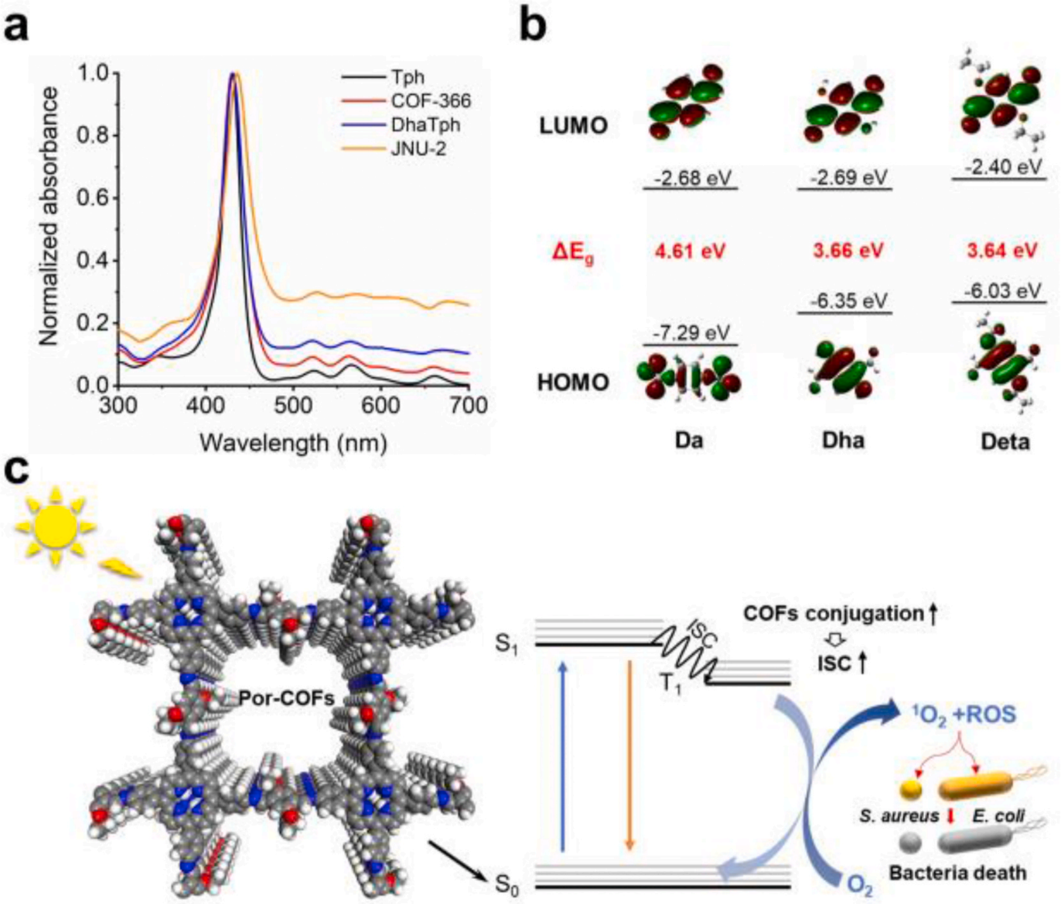

Fig. 4. (a) Normalized UV–vis absorption spectra of Por-COFs and Tph in THF. (b) Molecular orbital energy diagram of HOMO and LUMO for Da, Dha and Deta. (c) Possible mechanism for conjugation effect on photosensitizing activity of Por-COFs.

(TGA) also revealed the excellent thermal stability of the prepared Por-COFs up to ca. 400 °C under a N_2 atmosphere (Fig. S26-S28).

2.3. Photosensitizing activity of Por-COFs

The photosensitizing activity of the prepared Por-COFs was evaluated via monitoring decomposition of 9,10-anthracenediyl-bis(methylene)dimalonic acid (ABDA) by their produced singlet oxygen. As shown in Fig. 3, the monomer Tph gave slight decomposition of ABDA (29.8%) after 60 min irradiation with white LED light due to its self-aggregation. In contrast, COF-366 had 56.2% of ABDA degrade owing to the immobilization of Tph in its ordered structure, while DhaTph and JNU-2 led to much more significant decomposition of ABDA (73.2% and 100%, respectively) (Table S2). The degradation of ABDA in the presence of the three Por-COFs follows pseudo-first-order kinetics (Fig. 3c). The larger rate constant of JNU-2 (0.021 $\min^{-1}$) than COF-366 (0.010 $\min^{-1}$) and DhaTph (0.014 $\min^{-1}$) indicates the highest photosensitizing activity of JNU-2 (Table S3). JNU-2 still preserved its high ability in the decomposition of ABDA (>85%) after four runs, confirming the great photostability and reusability of Por-COFs (Fig. 3d).

The singlet oxygen quantum yield (Φ_Δ) relating to the efficiency of singlet oxygen generation of Por COFs in PBS was further determined with ABDA as indicator and Rose Bengal (RB) as the standard photosensitizer [36]. COF-366 gave a much lower Φ_Δ (0.23) than DhaTph (0.35) and JNU-2 (0.53) (Table S4), further implying the promotion of the enhanced conjugation for singlet oxygen generation of Por-COFs. The lager Φ_Δ of JNU-2 than various of previous photosensitizers including metal organic frameworks, COFs and graphene-based materials makes it great potential photosensitizer for diverse application (Table S5).

2.4. Mechanism of conjugation effect on photosensitizing activity of Por-COFs

We further investigated the mechanism of conjugation effect on photosensitizing activity. Enhancing molecule conjugation reduces the energy and increases the possibility of electron transition, resulting in the red-shift and broader spectral response of UV–vis absorption wavelength [37]. The UV–vis absorption spectra of all the Por-COFs display similar shape to that of Tph (typical Soret band at 430 nm and three Q-bands at 500–700 nm) (Fig. 4a). Compared with COF-366, DhaTph gave small broadening, while JNU-2 exhibited obvious red-shift as well as the broadening of the Soret band (Fig. 4a). Moreover, DhaTph and JNU-2 also had a red-shift in the fluorescence emission spectra compared with COF-366 (Fig. S29), indicating the higher conjugation of DhaTph and JNU-2 than COF-366. The larger intensity of the Q-bands (500–700 nm) of JNU-2 proves the higher conjugation of JNU-2 than DhaTph and COF-366 (Fig. 4a).

It was reported that conjugated monomers could increase the conjugation of 2D materials after the formation of two-dimensionally extended π-conjugated structure [30–32]. So, the conjugation of 2D COFs could be regulated with its building monomer. The geometry of the building monomer (Tph, Da, Dha, and Deta) was optimized based on the density functional theory calculation at a B3LYP/6-31G level to observe their frontier molecular orbitals of highest occupied molecular orbital (HOMO) and lowest unoccupied molecular orbital (LUMO) and the distribution of their delocalized electrons (Fig. 4b and Fig. S30). The lower calculated energy gap between the HOMO and LUMO (ΔE_g) of

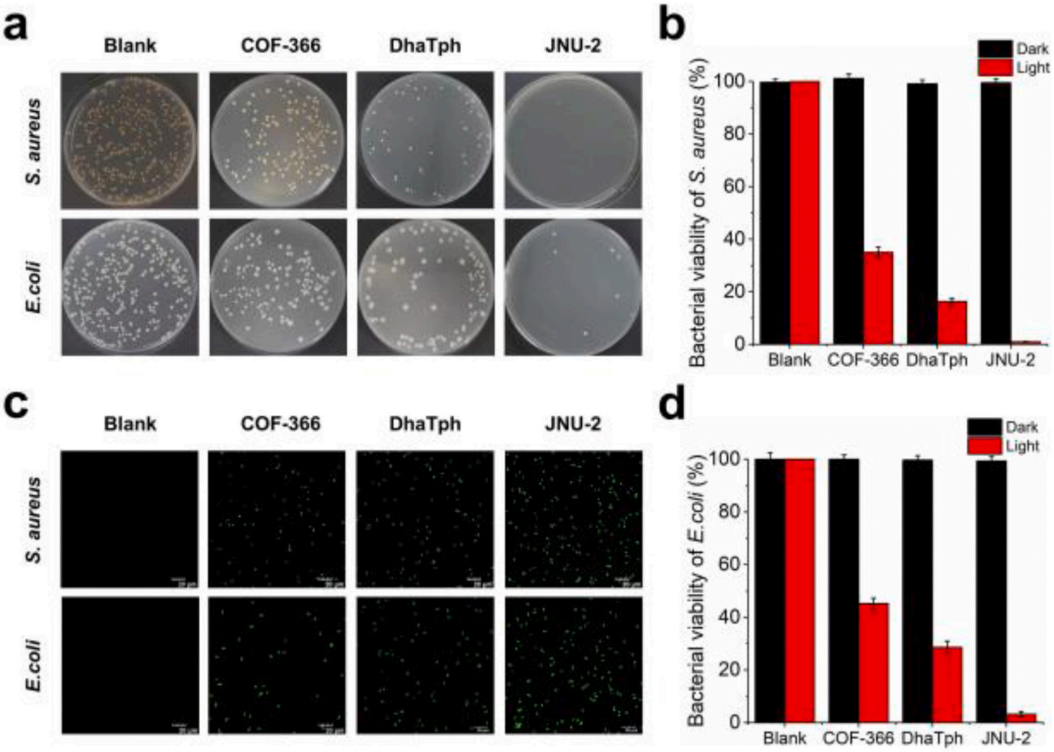

Fig. 5. (a) Photographs of bacterial colonies (10^4 times dilution) treated with Por-COFs under white LED light irradiation. (b) *S. aureus* viability of Por-COFs either with white LED irradiation or not. (c) Representative CLSM images for DCFH-DA stained bacteria either with Por-COFs or not. (d) *E. coli* viability of Por-COFs either with white LED irradiation or not. Blank experiments were performed without Por-COFs.

Dha (3.66 eV) and Deta (3.64 eV) than Da (4.61 eV) proved the more efficiency of electron transfer, indicating higher conjugation of Dha and Deta (Fig. 4b). Hence, DhaTph and JNU-2 consisting of Dha and Deta, respectively, possessed higher conjugation than COF-366. More importantly, the hydroxyl group of Dha can form intralayer H-bonding with the imine during the formation of COFs to limit intralayer flipping of DhaTph, and trigger extended π-cloud delocalization of DhaTph, which further enhances the conjugation of DhaTph (Fig. 1). The oxygen lone pairs of electrons donating ethoxy groups in Deta with lowest ΔE_g directly form intralayer p-π conjugation in JNU-2, resulting in the highest conjugation of JNU-2 in all the prepared Por-COFs (Fig. 1). The decrease of the higher-lying state (Tn and Sn) energy with the extension of conjugation in Por-COFs makes them get closer to their lowest state (T1 and S1), which causes the increase of ISC process and further improves the photosensitizing activity of Por-COFs (Fig. 4c) [38–41].

2.5. *Por-COFs in inactivation of bacteria*

The antibacterial activity of the prepared Por-COFs was evaluated against the two representative pathogens *Staphylococcus aureus* (*S. aureus*) and *Escherichia coli* (*E. coli*). Gram-positive *S. aureus* and gram-negative *E. coli* widely exist in food, water, human body wounds, and cause various illnesses to threaten human health [42]. The bacterial viability was evaluated by measuring the ratio of colony-forming units (CFU) counts for bacteria ($\sim 10^6$ CFU mL^{-1}) before and after treatment. No obvious bacteria death was observed under light irradiation alone (without Por-COFs) or in the presence of Por-COFs only (without light irradiation), indicating no phototoxicity and dark toxicity of Por-COFs (Fig. 5; Fig. S31-S32). Por-COFs in combination with a white LED light irradiation led to the significant decrease in the viability of *S. aureus* and *E. coli* (Fig. 5a, b and 5d). The 30-min incubation of JNU-2 (0.1 mg mL^{-1}) in combination with 20-min irradiation of 150 mW cm^{-2} white LED light resulted in the death of *S. aureus* (99.1%) and *E. coli* (96.8%) (Fig. S33-S38). In contrast, the same conditions for COF-366 and DhaTph resulted in only 65.0 and 83.7% death of *S. aureus*, and 55.8 and 71.5% death of *E. coli*, respectively (Fig. 5b and d). The relatively lower antibacterial activity of Por-COFs for *E. coli* than *S. aureus* accounted for the protection of unique membrane structure of gram-negative bacteria [43]. Moreover, the PXRD patterns of COF-366 and DhaTph reveal the obvious decrease of the crystallinity after the photodynamic inactivation of bacteria, while the maintenance of main PXRD peaks for JNU-2 indicates little effect of the photodynamic inactivation process on the crystalline structure of JNU-2 (Fig. S39). The highest efficiency of JNU-2 in inactivating *S. aureus* and *E. coli* among the three Por-COFs positively correlated with their photosensitizing activity, indicating the availability of conjugation-regulating strategy for designing Por-COFs with high photodynamic inactivation of bacteria.

The inactivation of bacteria by the singlet oxygen produced from Por-COFs was further confirmed by confocal laser scanning microscopy (CLSM). Singlet oxygen can oxidize nonfluorescent 2′,7′-dichlorodihydrofluorescein diacetate (DCFH-DA) into fluorescent dichlorofluoresce (DCF). Consequently, DCFH-DA was applied to indicate the generation of singlet oxygen in bacteria according to its fluorescence change. No fluorescence in *S. aureus* and *E. coli* was observed without incubation with Por-COFs (Fig. 5a and c), indicating no intracellular singlet oxygen in the bacteria and no bacteria death in the absence of Por-COFs. However, the bacteria treated with Por-COFs under white LED light irradiation showed obvious green fluorescence, indicating that Por-COFs produced singlet oxygen to inactive the *S. aureus* and *E. coli*. Moreover, the more significant fluorescence of the bacteria treated with JNU-2 than COF-366 and DhaTph also demonstrates the highest singlet oxygen yield of JNU-2. The significant photodynamic inactivation of JNU-2 confirms the high potential of Por-COFs in sterilization.

3. Conclusions

In conclusion, we have successfully developed a conjugation-regulating strategy for the synthesis of highly crystalline and stable

Por-COFs with dramatical singlet oxygen generation as photosensitizer in photodynamic inactivation of bacteria. The higher conjugation of Dha and Deta with lower ΔE_g led to the higher conjugation of DhaTph and JNU-2, respectively. Moreover, the hydroxyl group in Dha and the ethoxy groups in Deta further expanded the conjugation of DhaTph and JNU-2 via the formation of intralayer extended π-cloud delocalization and p-π conjunction, respectively. The extension of conjugation in DhaTph and JNU-2 improved their photosensitizing activity. The obtained JNU-2 with the highest photosensitizing activity exhibited superior antibacterial effects toward two widely existed bacteria (*S. aureus* and *E. coli*). This work offers a new conjugation-regulating strategy for designing high photosensitizing activity of Por-COFs and will largely expand the potential of Por-COFs in diverse application.

Credit author statement

Fan-Lin Meng: Methodology, Data curation, Writing-Original draft preparation. **Hai-Long Qian:** Conceptualization, Supervision, Funding acquisition, Writing-Reviewing and Editing. **Xiu-Ping Yan**： Funding acquisition, Resources, Supervision, Writing-Reviewing and Editing.

Declaration of competing interest

The authors declare that they have no known competing financial interests or personal relationships that could have appeared to influence the work reported in this paper.

Acknowledgment

Thanks for the supporting from the National Natural Science Foundation of China (No. 21804055, 21775056 and 22076066), the Natural Science Foundation of Jiangsu Province (No. BK20180585), the Fundamental Research Funds for the Central Universities (No. JUSRP221002), the National First-class Discipline Program of Food Science and Technology (No. JUFSTR20180301), the Program of “Collaborative Innovation Center of Food Safety and Quality Control in Jiangsu Province”.

Appendix A. Supplementary data

Supplementary data to this article can be found online at https://doi.org/10.1016/j.talanta.2021.122536.

References

[1] A.H. Havelaar, M.D. Kirk, P.R. Torgerson, H.J. Gibb, T. Hald, R.J. Lake, N. Praet, D. C. Bellinger, N.R. De Silva, N. Gargouri, N. Speybroeck, A. Cawthorne, C. Mathers, C. Stein, F.J. Angulo, B. Devleesschauwer, World Health Organization Foodborne Disease Burden Epidemiology Reference Group, World health organization global estimates and regional comparisons of the burden of foodborne disease in 2010, PLoS Med. 12 (12) (2015), e1001923.
[2] B.M. Peters, M.A. Jabra-Rizk, G.A. O'May, J.W. Costerton, M.E. Shirtliff, Polymicrobial interactions: impact on pathogenesis and human disease, Clin. Microbiol. Rev. 25 (1) (2012) 193–213.
[3] J.M.A. Blair, M.A. Webber, A.J. Baylay, D.O. Ogbolu, L.J.V. Piddock, Molecular mechanisms of antibiotic resistance, Nat. Rev. Microbiol. 13 (1) (2015) 42–51.
[4] S. Kandambeth, V. Venkatesh, D.B. Shinde, S. Kumari, A. Halder, S. Verma, R. Banerjee, Self-templated chemically stable hollow spherical covalent organic framework, Nat. Commun. 6 (2015) 6786.
[5] A.F. Silva, A. Borges, E. Giaouris, J.M.G. Mikcha, M. Simoes, Photodynamic inactivation as an emergent strategy against foodborne pathogenic bacteria in planktonic and sessile states, Crit. Rev. Microbiol. 44 (6) (2018) 667–684.
[6] S. Kwiatkowski, B. Knap, D. Przystupski, J. Saczko, E. Kedzierska, K. Knap-Czop, J. Kotlinska, O. Michel, K. Kotowski, J. Kulbacka, Photodynamic therapy - mechanisms, photosensitizers and combinations, Biomed. Pharmacother. 106 (2018) 1098–1107.
[7] F. Cieplik, D. Deng, W. Crielaard, W. Buchalla, E. Hellwig, A. Al-Ahmad, T. Maisch, Antimicrobial photodynamic therapy - what we know and what we don't, Crit. Rev. Microbiol. 44 (5) (2018) 571–589.
[8] V.S. Ghate, W.B. Zhou, H.G. Yuk, Perspectives and trends in the application of photodynamic inactivation for microbiological food safety, Compr. Rev. Food Sci. Food Saf. 18 (2) (2019) 402–424.
[9] A.F. Uchoa, K.T. de Oliveira, M.S. Baptista, A.J. Bortoluzzi, Y. Iamamoto, O. A. Serra, Chlorin photosensitizers sterically designed to prevent self-aggregation, J. Org. Chem. 76 (21) (2011) 8824–8832.
[10] R.F. Pasternack, C. Fleming, S. Herring, P.J. Collings, J. dePaula, G. DeCastro, E. J. Gibbs, Aggregation kinetics of extended porphyrin and cyanine dye assemblies, Biophys. J. 79 (1) (2000) 550–560.
[11] A.L. Tessaro, V.R. Batistela, A.C. Gracetto, H.P.M. de Oliveira, R.L. Sernaglia, V. R. de Souza, W. Caetano, N. Hioka, Stability of benzoporphyrin photosensitizers in water/ethanol mixtures: pKa determination and self-aggregation processes, J. Phys. Org. Chem. 24 (2) (2011) 155–161.
[12] J.V. Hollingsworth, A.J. Richard, M.G.H. Vicente, P.S. Russo, Characterization of the self-assembly of meso-tetra(4-sulfonatophenyl)porphyrin (H2TPPS4-) in aqueous solutions, Biomacromolecules 13 (1) (2012) 60–72.
[13] J.L. Segura, M.J. Mancheno, F. Zamora, Covalent organic frameworks based on Schiff-base chemistry: synthesis, properties and potential applications, Chem. Soc. Rev. 45 (20) (2016) 5635–5671.
[14] N. Huang, P. Wang, D.L. Jiang, Covalent organic frameworks: a materials platform for structural and functional designs, Nat. Rev. Mater. 1 (10) (2016) 16068.
[15] C.S. Diercks, O.M. Yaghi, The atom, the molecule, and the covalent organic framework, Science 355 (6328) (2017), eaal1585.
[16] M.S. Lohse, T. Bein, Covalent organic frameworks: structures, synthesis, and applications, Adv. Funct. Mater. 28 (33) (2018) 1705553.
[17] S. Cao, B. Li, R. Zhu, H. Pang, Design and synthesis of covalent organic frameworks towards energy and environment fields, Chem. Eng. J. 355 (2019) 602–623.
[18] A. Esrafili, A. Wagner, S. Inamdar, A.P. Acharya, Covalent organic frameworks for biomedical applications, Adv. Healthc. Mater. 10 (2021) 2002090.
[19] S. Lin, C.S. Diercks, Y.B. Zhang, N. Kornienko, E.M. Nichols, Y. Zhao, A.R. Paris, D. Kim, P. Yang, O.M. Yaghi, C.J. Chang, Covalent organic frameworks comprising cobalt porphyrins for catalytic CO2 reduction in water, Science 349 (6253) (2015) 1208–1213.
[20] X. Zhang, K.N. Chi, D.L. Li, Y. Deng, Y.C. Ma, Q.Q. Xu, R. Hu, Y.H. Yang, 2D-porphrinic covalent organic framework-based aptasensor with enhanced photoelectrochemical response for the detection of C-reactive protein, Biosens. Bioelectron. 129 (2019) 64–71.
[21] K. Wang, D.D. Qi, Y.L. Li, T.Y. Wang, H.B. Liu, J.Z. Jiang, Tetrapyrrole macrocycle based conjugated two-dimensional mesoporous polymers and covalent organic frameworks: from synthesis to material applications, Coord. Chem. Rev. 378 (2019) 188–206.
[22] B.P. Biswal, S. Valligatla, M. Wang, T. Banerjee, N.A. Saad, B.M.K. Mariserla, N. Chandrasekhar, D. Becker, M. Addicoat, I. Senkovska, R. Berger, D.N. Rao, S. Kaskel, X.L. Feng, Nonlinear optical switching in regioregular porphyrin covalent organic frameworks, Angew. Chem. Int. Ed. 58 (21) (2019) 6896–6900.
[23] Q. Guan, L.L. Zhou, Y.A. Li, W.Y. Li, S. Wang, C. Song, Y.B. Dong, Nanoscale covalent organic framework for combinatorial antitumor photodynamic and photothermal therapy, ACS Nano 13 (11) (2019) 13304–13316.
[24] V.-N. Nguyen, A. Kumar, M.H. Lee, J. Yoon, Recent advances in biomedical applications of organic fluorescence materials with reduced singlet–triplet energy gaps, Coord. Chem. Rev. 425 (2020) 13304.
[25] X.K. Chen, D. Kim, J.L. Bredas, Thermally activated delayed fluorescence (TADF) path toward efficient electroluminescence in purely organic materials: molecular level insight, Acc. Chem. Res. 51 (9) (2018) 2215–2224.
[26] H.V. Babu, M.G.M. Bai, M.R. Rao, Functional pi-conjugated two-dimensional covalent organic frameworks, ACS Appl. Mater. Interfaces 11 (12) (2019) 11029–11060.
[27] R.F. Chen, J.L. Shi, Y. Ma, G.Q. Lin, X.J. Lang, C. Wang, Designed synthesis of a 2D porphyrin-based sp2 carbon-conjugated covalent organic framework for heterogeneous photocatalysis, Angew. Chem. Int. Ed. 58 (19) (2019) 6430–6434.
[28] S.J. Liu, H.K. Zhang, Y.Y. Li, J.K. Liu, L.L. Du, M. Chen, R.T.K. Kwok, J.W.Y. Lam, D.L. Phillips, B.Z. Tang, Strategies to enhance the photosensitization: polymerization and the donor-acceptor even-odd effect, Angew. Chem. Int. Ed. 57 (46) (2018) 15189–15193.
[29] S.D. Xu, Y.Y. Yuan, X.L. Cai, C.J. Zhang, F. Hu, J. Liang, G.X. Zhang, D.Q. Zhang, B. Liu, Tuning the singlet-triplet energy gap: a unique approach to efficient photosensitizers with aggregation-induced emission (AIE) characteristics, Chem. Sci. 6 (10) (2015) 5824–5830.
[30] S. He, B. Yin, H. Niu, Y. Cai, Targeted synthesis of visible-light-driven covalent organic framework photocatalyst via molecular design and precise construction, Appl. Catal., B 239 (2018) 147–153.
[31] R. Xue, H. Guo, T. Wang, L. Gong, Y. Wang, J. Ai, D. Huang, H. Chen, W. Yang, Fluorescence properties and analytical applications of covalent organic frameworks, Anal. Methods 9 (25) (2017) 3737–3750.
[32] M.W. Lee, J.Y. Kim, H.J. Son, J.Y. Kim, B. Kim, H. Kim, D.K. Lee, K. Kim, D.H. Lee, M.J. Ko, Tailoring of energy levels in D-pi-A organic dyes via fluorination of acceptor units for efficient dye-sensitized solar cells, Sci. Rep. 5 (2015) 7711.
[33] S. Wan, F. Gándara, A. Asano, H. Furukawa, A. Saeki, S.K. Dey, L. Liao, M. W. Ambrogio, Y.Y. Botros, X. Duan, S. Seki, J.F. Stoddart, O.M. Yaghi, Covalent organic frameworks with high charge carrier mobility, Chem. Mater. 23 (18) (2011) 4094–4097.
[34] X. Chen, M. Addicoat, E. Jin, L. Zhai, H. Xu, N. Huang, Z. Guo, L. Liu, S. Irle, D. Jiang, Locking covalent organic frameworks with hydrogen bonds: general and remarkable effects on crystalline structure, physical properties, and photochemical activity, J. Am. Chem. Soc. 137 (9) (2015) 3241–3247.
[35] H. Xu, J. Gao, D. Jiang, Stable, crystalline, porous, covalent organic frameworks as a platform for chiral organocatalysts, Nat. Chem. 7 (11) (2015) 905–912.
[36] M. Hoebeke, X. Damoiseau, Determination of the singlet oxygen quantum yield of bacteriochlorin a: a comparative study in phosphate buffer and aqueous dispersion

of dimiristoyl-L-alpha-phosphatidylcholine liposomes, Photochem. Photobiol. Sci. 1 (4) (2002) 283–287.

[37] H. Meier, U. Stalmach, H. Kolshorn, Effective conjugation length and UV/vis spectra of oligomers, Acta Polym. 48 (9) (1997) 379–384.

[38] K. Schmidt, S. Brovelli, V. Coropceanu, D. Beljonne, J. Cornil, C. Bazzini, T. Caronna, R. Tubino, F. Meinardi, Z. Shuai, J.L. Bredas, Intersystem crossing processes in nonplanar aromatic heterocyclic molecules, J. Phys. Chem. A 111 (42) (2007) 10490–10499.

[39] S. Cekli, R.W. Winkel, E. Alarousu, O.F. Mohammed, K.S. Schanze, Triplet excited state properties in variable gap pi-conjugated donor-acceptor-donor chromophores, Chem. Sci. 7 (6) (2016) 3621–3631.

[40] J.Z. Zhao, W.H. Wu, J.F. Sun, S. Guo, Triplet photosensitizers: from molecular design to applications, Chem. Soc. Rev. 42 (12) (2013) 5323–5351.

[41] S. Cekli, R.W. Winkel, K.S. Schanze, Effect of oligomer length on photophysical properties of platinum acetylide donor-acceptor-donor oligomers, J. Phys. Chem. A 120 (28) (2016) 5512–5521.

[42] M.A. Noble, Bacteria in Biology, Biotechnology and Medicine, fourth ed., John Wiley & Sons, Chichester, 2007.

[43] A.M. Durantini, D.A. Heredia, J.E. Durantini, E.N. Durantini, BODIPYs to the rescue: potential applications in photodynamic inactivation, Eur. J. Med. Chem. 144 (2018) 651–661.